Surface segregation of Si and its effect on oxygen adsorption on a γ-TiAl(111) surface from first principles

2009 J. Phys.: Condens. Matter 21 225005

(http://iopscience.iop.org/0953-8984/21/22/225005)

IOP Publishing Journal of Physics: Condensed Matter

J. Phys.: Condens. Matter **21** (2009) 225005 (7pp) doi:10.1088/0953-8984/21/22/225005

Surface segregation of Si and its effect on oxygen adsorption on a γ-TiAl(111) surface from first principles

Shi-Yu Liu[1], Jia-Xiang Shang[1], Fu-He Wang[2] and Yue Zhang[1]

[1] Key Laboratory of Aerospace Materials and Performance (Ministry of Education), School of Materials Science and Engineering, Beihang University, Beijing 100191, People's Republic of China

[2] Department of Physics, Capital Normal University, Beijing 100037, People's Republic of China

E-mail: shangjx@buaa.edu.cn

Received 1 January 2009, in final form 27 March 2009
Published 22 April 2009
Online at stacks.iop.org/JPhysCM/21/225005

Abstract

We perform first-principles calculations based on the density-functional theory to study the surface segregation of Si and its effect on the oxygen adsorption on a γ-TiAl(111) surface for a range of oxygen coverage $0 < \Theta \leqslant 1.0$ monolayer (ML). The calculated results show that the alloying Si atoms prefer occupying surface Ti sites to the sites in the bulk of γ-TiAl, which suggests the occurrence of Si surface segregation. When oxygen atoms adsorb on a pure γ-TiAl(111) surface, the most favorable sites are the adsorption sites with more Ti atoms as their nearest neighbors in the surface layer at all the calculated coverages and the interactions between adsorbed oxygen atoms are repulsive. However, when oxygen atoms adsorb on an Si-alloyed γ-TiAl(111) surface, the interactions between the adsorbed oxygen atoms are attractive at oxygen coverage $0 < \Theta \leqslant 1.0$ ML. Meanwhile, the interactions between O and Al atoms become stronger whereas those between O and Ti atoms become weaker relative to oxygen adsorbed on a pure γ-TiAl(111) surface. The atomic geometry and density of state are analyzed. The results show that the surface ripple of the top metal layer for oxygen on a pure γ-TiAl(111) surface is Ti upwards, while that for oxygen on an Si-alloyed γ-TiAl(111) surface is Al upwards at high oxygen coverage ($\Theta \geqslant 0.50$ ML). This effect of Si is of benefit to the nucleation of alumina, which is attributed to Si surface segregation and an increase of the surface Al:Ti ratio. This can help to explain why alloying the γ-TiAl(111) surface with Si could favor the formation of the Al_2O_3 scale at the first stage and result in good oxidation resistance in experiments.

(Some figures in this article are in colour only in the electronic version)

1. Introduction

The lightweight γ-TiAl based intermetallics exhibit a large number of outstanding properties such as high melting point, low density and high specific strength. Therefore they are being considered as prospective structural materials for applications in aerospace and automobile industries [1–3]. However, their oxidation resistance properties still need to be improved above 700 °C. This is due to the growth of a mixed oxide layer formed by competitive oxidation of the Ti and Al alloying elements [4–8], which prevents the formation of a continuous and dense α-alumina that would provide a more effective oxidation barrier in high temperature applications. Whether a dense protective layer of Al_2O_3 is formed or a fast growing scale depends on the local activities of the metals and the oxides, which are influenced mainly by the oxygen partial pressure, temperature and also by addition of alloying elements [9, 10]. In experimental research, the addition of Si was reported to decrease the oxidation rate [10, 11] and the implantation of Si also resulted

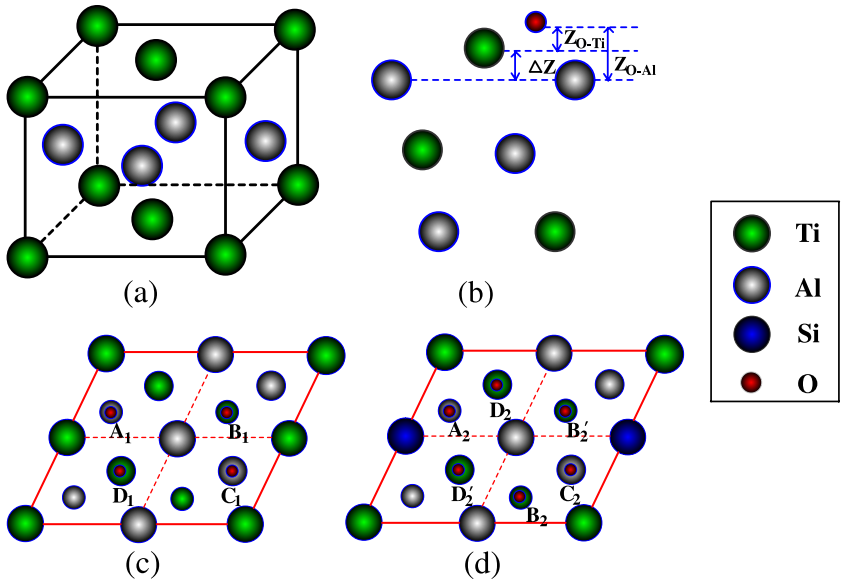

Figure 1. (a) The crystal structure of γ-TiAl bulk. (b) Schematic side view of the oxygen adsorbed γ-TiAl(111) surface. Top view of the γ-TiAl(111)-(2 × 2) surface models: (c) pure γ-TiAl(111) surface and (d) Si-alloyed γ-TiAl(111) surface, where one Si atom substitutes for one surface Ti atom indicated by a large blue ball. Large, medium, small green and gray balls represent surface, subsurface, the third layer Ti and Al, respectively, and the red one represents oxygen. The symbols A, B, C and D denote fcc-Al, fcc-Ti, hcp-Al and hcp-Ti sites, respectively. The subscript numbers 1 and 2 represent a pure γ-TiAl(111) surface and Si-alloyed γ-TiAl(111) surface, respectively. The superscript '′' in (d) denotes the same sites as that on the pure surface, but the surrounding atom in the first surface layer is changed from Ti to Si.

in excellent oxidation resistance, which is attributed to the formation of virtually Al_2O_3 layers in the scale during the initial stages of oxidation [12, 13].

On the theoretical side, Jiang *et al* [14] performed first-principles slab calculations based on the density-functional theory to investigate the surface segregation behavior of Pt on the clean (100), (110) and (111) surfaces of Ni_3Al. They found that the Pt has a strong tendency to segregate on these surfaces of Ni_3Al to substitute the surface Ni atom. It is the Pt surface segregation that increases the surface Al:Ni ratio, which kinetically favors the formation of Al_2O_3 over NiO. This thus helps to explain why Pt addition is beneficial to the oxidation resistance of Ni_3Al. Recently, Li *et al* [15] performed first-principles total energy calculations for oxygen adsorption on a pure γ-TiAl(111) surface. In our recent works, we studied oxygen adsorption on Ti(0001) [16] and Zr(0001) [17] surfaces from first principles. To our knowledge, however, the surface segregation of the alloying element as well as its effect on the oxygen adsorption on the γ-TiAl(111) surface has not been studied systematically. The purpose of this work is to achieve an understanding of Si surface segregation and its effect on oxygen adsorption on the γ-TiAl(111) surface from a microscopic point of view via *ab initio* density-functional calculation. The remainder of this paper is organized as follows. In section 2, we give the calculation details and calculation models. In section 3, the surface segregation behavior of Si on the γ-TiAl(111) surface is analyzed. Then the results of the Si surface segregation effect on the adsorption of oxygen on the γ-TiAl(111) surface are presented, where the energetics, atomic geometry and electronic properties are also analyzed. Finally, in section 4, our results are summarized.

2. Computational details and models

The present first-principles calculations are performed with the Vienna *ab initio* simulation package (VASP) [18–20] within the generalized gradient approximation (GGA) [21] using projector augmented wave (PAW) pseudopotentials [22, 23]. We tested k-point sampling and an energy cutoff convergence for all supercells. As a result of the convergence tests, we use an energy cutoff of 400 eV for all calculations.

The intermetallic compound γ-TiAl has a face-centered tetragonal (fct) $L1_0$ crystal structure with alternate (001) planes of Ti and Al atoms, which is shown in figure 1(a). The calculated lattice constants are $a = 3.980$ Å and $c = 4.086$ Å, which agree well with experiment [24] and previous DFT-GGA results [25]. For O/γ-TiAl(111) systems, they were modeled by a slab of seven metal slab layers separated by a vacuum region equivalent to seven bulk metal layers. The surface calculations were done in (2 × 2) surface unit cells with 9 × 9 × 1 Monkhorst–Pack k-points [26] in the Brillouin zone. Oxygen atom is placed on one side of the slab where the induced dipole moment is taken into account by applying a dipole correction [27, 28]. Here, the coverage of oxygen Θ is defined as the ratio of the number of adsorbed oxygen atoms to the number of atoms in an ideal substrate layer. In our calculations, the bottom three metal layers were fixed at their bulk truncated structure, the other atoms were relaxed until the forces on each of them were less than 0.01 eV $Å^{-1}$. To discuss the atomic structure clearly, a schematic side view of an adsorbed oxygen and the top three metal layers for the O/γ-TiAl(111) system is shown in figure 1(b).

We have calculated nine different adsorption sites (including top, bridge and hollow center sites) for oxygen on

the clean γ-TiAl(111)-(2×2) surface at a coverage of 0.25 ML. The calculated results show that the four sites fcc-Al, fcc-Ti, hcp-Al and hcp-Ti are much more stable than other sites. In the following, we just discuss the four sites as well as their combinations. The four oxygen adsorption sites are shown in figures 1(c) and (d), where the adsorption sites fcc-Al, fcc-Ti, hcp-Al and hcp-Ti are denoted by A, B, C and D, respectively. Figures 1(c) and (d) represent the adsorption sites on the pure γ-TiAl(111)-(2 × 2) surface and the Si-alloyed γ-TiAl(111)-(2 × 2) surface, in which one of the surface Ti atom is replaced by an Si atom, respectively. The subscript numbers 1 and 2 represent these two cases, and the prime ‘’ in figure 1(d) denotes the same sites as that on the pure surface, but one of the surrounding atoms in the first surface layer is changed from Ti to Si.

To calculate the defect formation energy and surface segregation energy, one Si atom substitutes one Ti (or Al) atom at the γ-TiAl(111)(2 × 2) surface unit cell and in the 2 × 2 × 2 32-atom bulk supercell.

The impurity formation energy of Si in the bulk and at the surface is defined as

$$E_{\text{imp}}^{\text{M}} = E_{\text{t}}^{\text{M-Si}} - E_{\text{t}}^{\text{M}} + E_{\text{X}}^{\text{bulk}} - E_{\text{Si}}^{\text{bulk}}, \quad (1)$$

where M represents the γ-TiAl(111) surface or γ-TiAl bulk, respectively; X represents the substituted atom; E_{t}^{M} and $E_{\text{t}}^{\text{M-Si}}$ represent the total energies of M and Si-doped M, respectively. $E_{\text{X}}^{\text{bulk}}$ and $E_{\text{Si}}^{\text{bulk}}$ represent the total energies per X and Si atom in their bulk states, respectively.

The tendency of an impurity atom to segregate to the surface can be characterized by the surface segregation energy E_{seg}, defined as

$$E_{\text{seg}} = E_{\text{imp}}^{\text{surf}} - E_{\text{imp}}^{\text{bulk}}, \quad (2)$$

where $E_{\text{imp}}^{\text{surf}}$ and $E_{\text{imp}}^{\text{bulk}}$ denote the impurity formation energy of Si at the surface and in the bulk, respectively. A negative E_{seg} indicates that it is energetically favorable for the impurity atom to segregate to the surface and vice versa.

The stability of various O/γ-TiAl(111) systems is analyzed with respect to the average binding energy per oxygen atom. The average binding energy per oxygen atom as a function of the coverage Θ is defined as

$$E_{\text{b}}(\Theta) = \frac{1}{N_{\text{O}}^{\text{atom}}}[E_{\text{O/TiAl(111)}}^{\text{slab}}(\Theta) - (E_{\text{TiAl(111)}}^{\text{slab}} + N_{\text{O}}^{\text{atom}} E_{\text{O}}^{\text{atom}})], \quad (3)$$

where $N_{\text{O}}^{\text{atom}}$ is the number of oxygen atoms in the unit cell, $E_{\text{O/TiAl(111)}}^{\text{slab}}$, $E_{\text{TiAl(111)}}^{\text{slab}}$ and $E_{\text{O}}^{\text{atom}}$ represent the total energies per unit cell of the TiAl(111) slab with oxygen atoms, the clean TiAl(111) slab, and free oxygen atom, respectively.

In order to roughly evaluate the interaction between the adsorbed oxygen atoms, we define an indirect interaction energy as

$$E_{\text{ind}}(\Theta) = E_{\text{b}}(\Theta) - \frac{1}{N_{\text{O}}^{\text{atom}}} \sum_i E_{\text{b}}^i(0.25), \quad (4)$$

where $E_{\text{b}}(\Theta)$ represents the binding energy at oxygen coverage Θ. $E_{\text{b}}^i(0.25)$ represents the binding energy per oxygen atom of the ith adsorption site at $\Theta = 0.25$ ML. The sum is over all the sites, which is involved when we calculate the $E_{\text{b}}(\Theta)$. The negative and positive values of E_{ind} correspond to an attractive and repulsive interaction between the adsorbed oxygen atoms, respectively.

Table 1. The calculated impurity formation energies E_{imp} (eV) of Si at the γ-TiAl(111) surface and bulk γ-TiAl and surface segregation energy E_{seg} (eV) of Si at the γ-TiAl(111) surface.

	E_{imp} (eV)	E_{imp} (eV)	E_{seg} (eV)	E_{seg} (eV)
Layer	Ti site	Al site	Ti site	Al site
1	−0.59	−0.46	−0.66	−0.10
2	0.12	−0.33	0.05	0.03
Bulk	0.07	−0.36		

3. Results and discussion

3.1. Surface segregation energy

In order to identify site preference of Si at the γ-TiAl(111) surface and in the γ-TiAl bulk, the impurity formation energies of Si both in the bulk and at the surface are calculated by equation (1). In the calculation, one of the Ti or Al atoms in the bulk and at surfaces is replaced by an Si atom. The calculated impurity formation energy and surface segregation energy at Ti or Al sites are listed in table 1. The impurity formation energies of Si substituting for Al and Ti atoms are negative and positive, respectively, when the substituted Al and Ti atoms are in the bulk or even in the subsurface layer. This indicates that only Al atoms in the bulk or under the surface can be substituted by Si atoms. This is consistent with the previous theoretical result [29]. However, the situation changes completely for the top surface: the impurity formation energy of Si substituting for Ti atom in the first surface layer is lower than that for Al atom, though the impurity formation energies of Si at Ti and Al sites are all negative. This indicates that the Si atoms prefer segregating to the top layer at the Ti site. The surface segregation energy calculated with equation (2) is also listed in table 1. For the first layer, the Si segregation energies are negative. But the magnitude is different: it is −0.66 eV and −0.10 eV for the Ti site and Al site, respectively, which indicates that the Si atom mainly substitutes for Ti atoms. This surface is denoted by an Si-alloyed γ-TiAl(111) surface. Therefore, further calculations on the Si-alloyed γ-TiAl(111) surface are based on the assumption that the Si atom substitutes for the Ti atom in the first surface layer in section 3.2. The Si surface segregation increases the surface Al:Ti ratio, which possibly favors the formation of Al_2O_3 over TiO_2 and improves the oxidation resistance property of TiAl [10–13] similar to the effect of Pt addition to the Ni_3Al surface [14].

3.2. Oxygen binding energy

As we know, oxygen adsorption on the surface is the first step of materials oxidation. To understand the microscopic mechanism of an *initio* oxidation process, the average binding

Table 2. The calculated binding energies per oxygen atom E_b (eV/atom) and indirect interaction energy E_{ind} (eV/atom) on a pure γ-TiAl(111) surface at different adsorption sites for a range of oxygen coverage $0 < \Theta \leqslant 1$.

Site	0.25 ML	Site	0.5 ML	E_{ind}	Site	0.75 ML	E_{ind}	Site	1.0 ML	E_{ind}
A_1	−8.36	$A_1 + A_1$	−8.23	0.13	$A_1 + A_1 + C_1$	−7.93	0.40	$A_1 + A_1 + C_1 + C_1$	−7.84	0.47
C_1	−8.26	$C_1 + C_1$	−8.18	0.08	$A_1 + A_1 + B_1$	−7.83	0.23	$A_1 + A_1 + B_1 + B_1$	−7.83	0.08
B_1	−7.46	$B_1 + B_1$	−7.87	−0.41	$C_1 + C_1 + D_1$	−7.78	0.20	$C_1 + C_1 + D_1 + D_1$	−7.72	0.11
D_1	−7.40	$D_1 + D_1$	−7.67	−0.27	$B_1 + B_1 + D_1$	−7.63	−0.19	$B_1 + B_1 + D_1 + D_1$	−7.63	−0.20
		$A_1 + C_1$	−8.36	−0.05						
		$A_1 + B_1$	−7.82	0.09						
		$C_1 + D_1$	−7.76	0.07						
		$B_1 + D_1$	−7.60	−0.17						

Table 3. The calculated binding energies E_b per oxygen atom (eV/atom) and indirect interaction energy E_{ind} (eV/atom) on an Si-alloyed γ-TiAl(111) surface at different adsorption sites for a range of oxygen coverage $0 < \Theta \leqslant 1$.

Site	0.25 ML	Site	0.5 ML	E_{ind}	Site	0.75 ML	E_{ind}	Site	1.0 ML	E_{ind}
A_2	−7.04	$A_2 + A_2$	−7.06	−0.02	$A_2 + A_2 + C_2$	−7.23	−0.16	$A_2 + A_2 + C_2 + C_2$	−7.33	−0.24
C_2	−7.14	$C_2 + C_2$	−7.10	0.04	$A_2 + A_2 + B_2$	−7.38	−0.11	$A_2 + A_2 + B_2 + B_2'$	−7.49	−0.53
B_2	−7.72	$B_2 + B_2'$	−7.21	−0.34	$C_2 + C_2 + D_2$	−7.41	−0.11	$C_2 + C_2 + D_2 + D_2'$	−7.54	−0.52
D_2	−7.63	$D_2 + D_2'$	−7.24	−0.33	$B_2 + B_2' + D_2$	−7.04	0.09	$B_2 + B_2' + D_2 + D_2'$	−7.24	−0.35
B_2'	−6.03	$A_2 + C_2$	−7.30	−0.12	$B_2 + D_2 + C_2$	−7.60	−0.10	$B_2 + D_2 + C_2 + A_2$	−7.49	−0.11
D_2'	−6.19	$A_2 + B_2$	−7.38	0.00						
		$A_2 + B_2'$	−7.02	−0.49						
		$C_2 + D_2$	−7.46	−0.08						
		$C_2 + D_2'$	−7.08	−0.42						
		$B_2 + D_2$	−7.83	−0.16						
		$B_2' + D_2'$	−6.41	−0.30						

energy per oxygen atom on the TiAl(111) surface at different coverage Θ is calculated by equation (3).

To study the effect of Si on the oxygen adsorption on the γ-TiAl(111) surface, we first calculate the average oxygen binding energies on the clean γ-TiAl(111) surface. The calculated oxygen binding energies at different oxygen coverages and adsorption sites are listed in table 2. From table 2, it can be found that for $\Theta = 0.25$ ML the most favorable site is the fcc-Al (A_1) site, followed by the hcp-Al (C_1) site, then fcc-Ti (B_1) and hcp-Ti (D_1) sites. It should be noticed that both fcc-Al (A_1) and hcp-Al (C_1) are the adsorption sites with more Ti atoms as nearest neighbors on the surface layer, while both fcc-Ti (C_1) and hcp-Ti (D_1) are the adsorption sites with more Al atoms as nearest neighbors on the surface layer. Turning to higher coverages, the combination of fcc-Al (A_1) and hcp-Al (C_1) is the most stable site for the oxygen coverage $0.50 \leqslant \Theta \leqslant 1.00$. Therefore, the adsorption sites with more Ti atoms as nearest neighbors on the surface layer are the most favorable sites for oxygen adsorption on the clean γ-TiAl(111) surface at all the calculated coverages. These results are in agreement with the previous theoretical result of Li *et al* [15]. From the oxygen binding energy, the indirect interaction energy calculated by equation (4) is also listed in table 2. It can be seen that the indirect interaction energies for the most stable configuration are positive (0.40 and 0.47 eV for $\Theta = 0.75$ and 1.0 ML), which means that strong repulsive interaction among the O atoms exists. It is negative only for the combination of fcc-Ti and hcp-Ti ($B_1 + B_1$, $D_1 + D_1$, $B_1 + D_1$, $B_1 + B_1 + D_1$, $B_1 + B_1 + D_1 + D_1$). For these adsorption sites, there are more Al atoms in their nearest neighbors.

In order to study the effect of Si on the adsorption of oxygen on the γ-TiAl(111) surface, we perform calculations about the oxygen adsorption on an Si-alloyed γ-TiAl(111) surface where one Si atom substitutes for a surface Ti site in a (2×2) supercell. In this case (see figure 1(d)), there are two Al atoms, one Si atom and one Ti atom in the top surface layer. Therefore, for oxygen adsorption there are two fcc-Al (A_2) sites, two fcc-Ti (B_2 and B_2') sites, two hcp-Al (C_2) and two hcp-Ti (D_2 and D_2') sites. The calculated oxygen binding energies at different oxygen coverages and adsorption sites are listed in table 3. From table 3, it can be found that for 0.25 ML the most favorable site is the fcc-Ti (B_2) site, followed by the hcp-Ti (D_2) site, then fcc-Al (C_2) and hcp-Al (A_2), hcp-Ti (D_2') and fcc-Ti (B_2') sites. It should be mentioned that both fcc-Ti (B_2) and hcp-Ti (D_2) sites are the adsorption sites with two Al atoms and one Ti atom as nearest neighbors on the surface layer, and both fcc-Ti (B_2') and hcp-Ti (D_2') sites are the adsorption sites with two Al atoms and one Si atom as their nearest sites, while both fcc-Al (C_2) and hcp-Al (A_2) are the adsorption sites with one Ti, one Al and one Si atom as their nearest neighbors on the surface layer. It can be seen clearly that the local composition has a strong effect on the oxygen adsorption behavior. At $\Theta = 0.50$ ML, the most favorable site is the combination of fcc-Ti (B_2) and hcp-Ti (D_2). Turning to higher coverages, the combination of $B_2 + D_2 + C_2$ and combination of $C_2 + C_2 + D_2 + D_2'$ are the most stable sites for the oxygen coverages $\Theta = 0.75$ and 1.00 ML, respectively. From further inspection of table 3, it is interesting to note that, for O/Si-alloyed γ-TiAl(111) systems, the indirect interaction energy (E_{ind}) of almost all configurations is negative, only being slightly positive for the combinations $C_2 + C_2$ at $\Theta = 0.50$ ML, $B_2 + B_2' + D_2$ at $\Theta = 0.75$ ML.

Table 4. The calculated structure parameters (in Å) for oxygen adsorption on both pure γ-TiAl(111) and Si-alloyed γ-TiAl(111) surfaces at the most stable sites for a range of oxygen coverage $0 \leqslant \Theta \leqslant 1$.

		Site	R_{O-Al}	R_{O-Ti}	Z_{O-Al}	Z_{O-Ti}	ΔZ
0.00 ML	γ-TiAl(111)						−0.173
	Si-alloyed γ-TiAl(111)						−0.217
0.25 ML	γ-TiAl(111)	fcc-Al	1.875	1.955	0.941	1.058	−0.117
	Si-alloyed γ-TiAl(111)	fcc-Ti	1.835	2.032	0.820	0.999	−0.179
0.50 ML	γ-TiAl(111)	fcc-Al	1.847	1.935	1.089	1.014	0.075
		hcp-Al	1.804	1.952	0.927	0.851	0.076
	Si-alloyed γ-TiAl(111)	fcc-Ti	1.823	2.002	0.890	0.944	−0.054
		hcp-Ti	1.802	2.046	0.922	0.977	−0.055
0.75 ML	γ-TiAl(111)	fcc-Al	1.864	1.901	1.232	0.883	0.349
		hcp-Al	1.756	1.973	1.011	0.661	0.350
	Si-alloyed γ-TiAl(111)	fcc-Ti	1.795	2.075	0.694	0.958	−0.264
		hcp-Ti	1.798	2.037	0.598	0.862	−0.264
		hcp-Al	1.863	2.092	0.283	0.547	−0.264
1.00 ML	γ-TiAl(111)	fcc-Al	1.823	1.932	1.440	0.789	0.651
		hcp-Al	1.742	1.942	0.946	0.295	0.651
	Si-alloyed γ-TiAl(111)	hcp-Al	1.806	2.082	0.536	1.150	−0.614
		hcp-Al	1.806	2.082	0.536	1.150	−0.614
		hcp-Ti	1.766	2.031	0.610	1.224	−0.614
		hcp-Ti	1.870	3.593	0.982	1.597	−0.615

The indirect interaction energies of the most stable configuration are all negative for $\Theta \geqslant 0.5$ ML, which indicates attractive interactions between adsorbed oxygen atoms. This may be beneficial for the formation of alumina islands.

3.3. Atomic structure

To investigate the Si effect on surface atomic structure, the atomic structures of the pure O/γ-TiAl(111) and O/Si-alloyed γ-TiAl(111) systems at the most stable sites with different oxygen coverage are listed in table 4. We calculate the minimal O–Ti separation and the minimal O–Al separation, both in three-dimensional space R_{O-Ti} and R_{O-Al} and along the direction normal to the surface Z_{O-Ti} and Z_{O-Al}. The surface ripple between Al and Ti in the first layer defined as $\Delta Z = Z_{Ti} - Z_{Al} = Z_{O-Al} - Z_{O-Ti}$ is also listed in table 4. For clarity, the schematic side view of the γ-TiAl(111) slab is shown in figure 1(b). The negative and positive values of ΔZ correspond to Al and Ti atoms' upward-facing surfaces, respectively.

From table 4, it can be seen clearly that the O–Al distances (R_{O-Al} and Z_{O-Al}) of O/Si-alloyed γ-TiAl(111) systems become shorter than that of O/γ-TiAl(111) systems. Meanwhile, the O–Ti distances (R_{O-Ti} and Z_{O-Ti}) of O/Si-alloyed γ-TiAl(111) systems become longer than that of O/γ-TiAl(111) systems. This indicates that, for O/Si-alloyed γ-TiAl(111) systems, the interaction between O and Al atoms becomes stronger and the interaction between O and Ti atoms becomes weaker relative to O/γ-TiAl(111) systems. Further inspection of table 4 shows that the surface ripples between Al and Ti (ΔZ) for clean pure γ-TiAl(111) and Si-alloyed γ-TiAl(111) surfaces are both negative, which indicates that the Al atom is higher than the Ti atom in the first surface layer. Furthermore, the surface layer ripples between Al and Ti (ΔZ) for O/γ-TiAl(111) systems increase from a negative value to a positive value with increasing oxygen coverage, which indicates that oxygen could induce the top layer from Al upwards to Ti upwards the oxygen coverage increases. For O/Si-alloyed γ-TiAl(111) systems, the surface layer ripples between Al and Ti (ΔZ) are all negative, which indicates that the Al atom is higher than the Ti atom in the first surface layer. When oxygen coverage is $\Theta = 0.75$ and 1.0 ML, the surface ripple can get to −0.26 and −0.61 Å, which indicates that the interaction between O and Al atoms is stronger than that between O and Ti atoms. This may be an indicator of the nucleation of alumina.

3.4. Density of states

In order to understand the Si alloying effect on the bonding behavior of an oxygen atom with the substrate, we also analyze our results by means of the projected density of states (PDOS). In this section, we mainly discuss the cases of the most stable oxygen adsorbed systems with coverages $\Theta = 0.25$, 0.50 and 1.00 ML. The PDOS of O/γ-TiAl(111) systems with 0.25, 0.50 and 1.00 ML are shown in figures 2(a), (c) and (e), respectively. The PDOS of O/Si-alloyed γ-TiAl(111) systems with 0.25, 0.50 and 1.00 ML are shown in figures 2(b), (d) and (f), respectively.

For oxygen coverage of 0.25 ML, O_{2p} states interact with Al_{3p} and $Ti_{4p,3d}$ at about −4.7 eV; O_{2s} states interact with $Al_{3s,3p}$ and $Ti_{4s,4p,3d}$ at about −18.8 eV for the O/γ-TiAl(111) (figure 2(a)) system. However, when an oxygen atom is adsorbed on an Si-alloyed γ-TiAl(111) surface (figure 2(b)), the O_{2p} states split into two peaks at about −4.3 and −6.3 eV. Besides the interactions between O_{2p} and Al_{3p} states at −4.3 eV as existed in the O/γ-TiAl(111) system, there are interactions between O_{2p} and Al_{3s} at −6.3 eV. As a result, the interactions between O and Al atoms in the O/Si-alloyed γ-TiAl(111) system are stronger than those in the O/γ-TiAl(111) system.

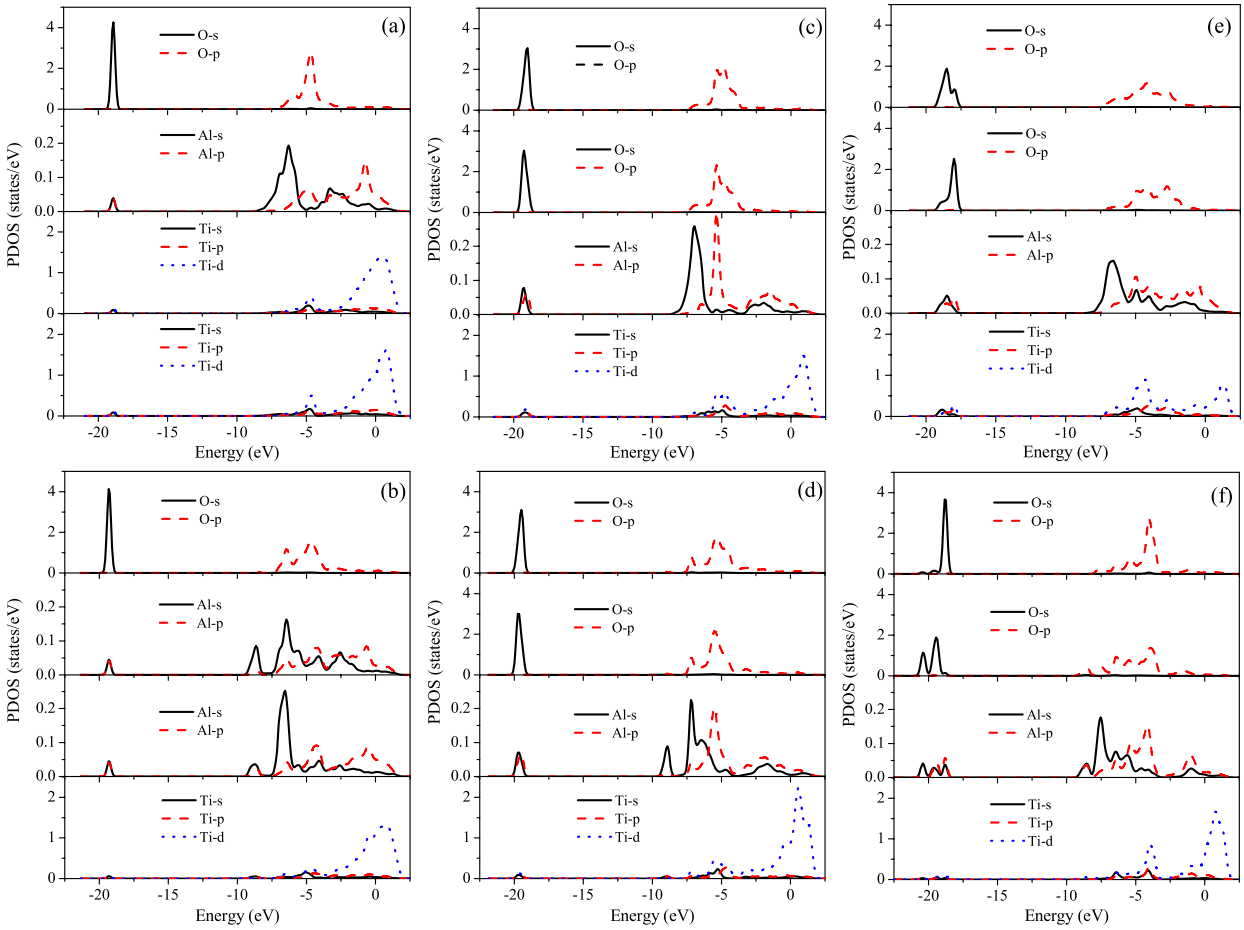

Figure 2. The projected density of states for the systems O/γ-TiAl(111) with 0.25 ML (a), 0.50 ML (c) and 1.00 ML (e) as well as O/Si-alloyed γ-TiAl(111) with 0.25 ML (b), 0.50 ML (d) and 1.00 ML (f) at the most stable site. The s, p and d states are indicated by solid, dashed and dotted lines. The zero energy corresponds to the Fermi level.

Turning to the high coverage of 0.50 and 1.00 ML, similar features can be found as discussed for the coverage of 0.25 ML above. For the O/γ-TiAl(111) (figures 2(c) and (e)) system, O_{2p} states interact with Al_{3p} and $Ti_{4p,3d}$ in the energy range from -1.5 to -7.0 eV; O_{2s} states interact with $Al_{3s,3p}$ and $Ti_{4s,4p,3d}$ at about -18 eV. For the O/Si-alloyed γ-TiAl(111) (figures 2(d) and (f)) system, two peaks appear at about -5.0 and -7.8 eV in O_{2p} states. The states of O_{2p} strongly interact with Al_{3s} and Al_{3p} states at these energy levels. The O_{2s} states at a lower energy level of -20.0 eV interact with states of $Al_{3s,3p}$. The energy levels for the O/Si-alloyed γ-TiAl(111) system (see figures 2(d) and (f)) are shifted downward compared with those of the O/γ-TiAl(111) system (see figures 2(c) and (e)), which also indicates that the interactions between O and Al atoms are stronger than those in the O/γ-TiAl(111) system. For the PDOS of O/Si-alloyed γ-TiAl(111) systems as shown in figures 2(b), (d) and (f), we can also find that the bonding between O and Al becomes stronger with the increase of the oxygen coverage, which is consistent with the above result from the atomic structure analysis.

4. Summary and conclusion

Using density-functional theory, we have studied surface segregation of Si as well as its effect on the adsorption of oxygen on a γ-TiAl(111) surface. Our calculated results show that Si atoms prefer segregating on the γ-TiAl(111) surface, substituting for surface Ti atoms, which thus increases the surface Al:Ti ratio. For oxygen adsorption on a pure γ-TiAl(111) surface, the interactions between adsorbed O atoms at the most stable sites are repulsive at oxygen coverage $\Theta \geqslant 0.50$ ML. However, for oxygen adsorption on an Si-alloyed γ-TiAl(111) surface, the interactions between adsorbed O atoms at the most stable sites are attractive, which may be beneficial for the nucleation of alumina. The atomic structures are analyzed. At oxygen coverage $\Theta \geqslant 0.5$ ML, the surface ripple of the top metal layer for oxygen on a pure γ-TiAl(111) surface is Ti upwards, while that for oxygen on an Si-alloyed γ-TiAl(111) surface is Al upwards. The results of PDOS also indicate that the interaction between O and Al atoms becomes stronger because of the Si surface segregation effect. As a result, the surface segregation of Si at the γ-TiAl(111) surface could result in good oxidation resistance for γ-TiAl as found in experiments.

Acknowledgments

This work was supported by the Foundation for National Excellent Doctoral Dissertations of China under grant

No. 200334 and by the National Natural Science Foundation of China under grant No. 50871071.

References

[1] Froes F H, Suryanarayana C and Eliezer D 1992 *J. Mater. Sci.* **27** 5113
[2] Loria E A 2000 *Intermetallics* **8** 1339
[3] Clemens H and Kestler H 2000 *Adv. Eng. Mater.* **2** 551
[4] Rahmel A, Quadakkers W J and Schütze M 1995 *Mater. Corros.* **46** 217
[5] Becker S, Rahmel A, Schorr M and Schütze M 1992 *Oxid. Met.* **38** 425
[6] Lang C and Schütze M 1996 *Oxid. Met.* **46** 255
[7] Lang C and Schütze M 1997 *Mater. Corros.* **48** 13
[8] Schmitz-Niederau M and Schütze M 1999 *Oxid. Met.* **52** 225
[9] Maki K, Shioda M, Sayashi M, Shimizu T and Isobe S 1992 *Mater. Sci. Eng.* A **153** 591
[10] Shida Y and Anada H 1994 *Mater. Trans. JIM* **35** 623
[11] Kim B G, Kim G M and Kim C J 1995 *Scr. Metall. Mater.* **33** 1117
[12] Taniguchi S, Uesaki K, Zhu Y C, Matsumoto Y and Shibata T 1999 *Mater. Sci. Eng.* A **266** 267
[13] Taniguchi S, Kuwagawa T, Zhu Y C, Matsumoto Y and Shibata T 2000 *Mater. Sci. Eng.* A **277** 229
[14] Jiang C and Gleeson B 2007 *Acta Mater.* **55** 1641
[15] Li H, Liu L M, Wang S Q and Ye H Q 2006 *Acta Metall. Sin.* **42** 897
[16] Liu S Y, Wang F H, Zhou Y S and Shang J X 2007 *J. Phys.: Condens. Matter* **19** 226004
[17] Wang F H, Liu S Y, Shang J X, Zhou Y S, Li Z Y and Yang J L 2008 *Surf. Sci.* **602** 2212
[18] Kresse G and Hafner J 1993 *Phys. Rev.* B **48** 13115
[19] Kresse G and Furthmüller J 1996 *Phys. Rev.* B **54** 11169
[20] Kresse G and Furthmüller J 1996 *Comput. Mater. Sci.* **6** 15
[21] Perdew J P, Chevary J A, Vosko S H, Jackson K A, Pederson M R, Singh D J and Fiolhais C 1992 *Phys. Rev.* B **46** 6671
[22] Blöchl P E 1994 *Phys. Rev.* B **50** 17953
[23] Kresse G and Joubert D 1999 *Phys. Rev.* B **59** 1758
[24] Brandes E A 1983 *Smithell Metals Reference Book* 6th edn (London: Butterworth)
[25] Benedek R, van de Walle A, Gerstl S S A, Asta M, Seidman D N and Woodward C 2005 *Phys. Rev.* B **71** 094201
[26] Monkhorst H J and Pack J D 1976 *Phys. Rev.* B **13** 5188
[27] Neugebauer J and Scheffler M 1992 *Phys. Rev.* B **46** 16067
[28] Bengtsson L 1999 *Phys. Rev.* B **59** 12301
[29] Woodward C, Kajihara S and Yang L H 1998 *Phys. Rev.* B **57** 13459